WATER RESEARCH 46 (2012) 4633–4644

Available online at www.sciencedirect.com

SciVerse ScienceDirect

journal homepage: www.elsevier.com/locate/watres

Heterogeneous UV/Fenton degradation of TBBPA catalyzed by titanomagnetite: Catalyst characterization, performance and degradation products

Yuanhong Zhong [a,c], Xiaoliang Liang [a,c], Yin Zhong [b], Jianxi Zhu [a], Sanyuan Zhu [a], Peng Yuan [a], Hongping He [a,*], Jing Zhang [d]

[a] Key Laboratory of Mineralogy and Metallogeny, Guangzhou Institute of Geochemistry, Chinese Academy of Sciences, 511 Kehua Street, Guangzhou 510640, China

[b] Pearl River Delta Research Center of Environment Pollution and Control, Guangzhou Institute of Geochemistry, Chinese Academy of Sciences, Guangzhou 510640, China

[c] Graduate University of the Chinese Academy of Sciences, Beijing 100049, China

[d] Institute of High Energy Physics, Chinese Academy of Sciences, Beijing 100049, China

ARTICLE INFO

Article history:
Received 20 December 2011
Received in revised form
24 May 2012
Accepted 13 June 2012
Available online 27 June 2012

Keywords:
Titanomagnetite
Substitution
Degradation
UV/Fenton
TBBPA

ABSTRACT

Tetrabromobisphenol A (TBBPA), a widely used brominated flame retardant, could negatively affect various aspects of mammalian and human physiology, which triggers effective techniques for its removal. In this work, the degradation characteristics of TBBPA in heterogeneous UV/Fenton reaction catalyzed by titanomagnetite ($Fe_{3-x}Ti_xO_4$) were studied. Batch tests were conducted to evaluate the effects of titanomagnetite dosage, H_2O_2 concentration and titanium content in magnetite on TBBPA degradation. In the system with 0.125 g L^{-1} of $Fe_{2.02}Ti_{0.98}O_4$ and 10 mmol L^{-1} of H_2O_2, almost complete degradation of TBBPA (20 mg L^{-1}) was accomplished within 240 min UV irradiation at pH 6.5. The titanium incorporation obviously enhanced the catalytic activity of magnetite. As shown by the XRD and XANES results, titanomagnetite had a spinel structure with Ti^{4+} occupying the octahedral sites. On the basis of the degradation products identified by GC-MS, the degradation pathways of TBBPA were proposed. TBBPA possibly underwent the sequential debromination to form TriBBPA, DiBBPA, MonoBBPA and BPA, and β-scission to generate seven brominated compounds. All of these products were finally completely removed from reaction solution. In addition, the reused catalyst $Fe_{2.02}Ti_{0.98}O_4$ still retained the catalytic activity after three cycles, indicating that titanomagnetite had good stability and reusability. These results demonstrated that heterogeneous UV/Fenton reaction catalyzed by titanomagnetite is a promising advanced oxidation technology for the treatment of wastewater containing TBBPA.

1. Introduction

Tetrabromobisphenol A (TBBPA) is one of the most important brominated flame retardants (BFRs) widely used in printed circuit boards, insulated wires and various polycarbonate plastics (Kitamura et al., 2002). Due to its extensive usage, TBBPA has been detected in various environmental matrices, including sediment (Voordeckers et al., 2002), biological

* *Corresponding author*. Tel.: +86 20 85290257; fax: +86 20 85290130.
E-mail address: hehp@gig.ac.cn (H. He).
0043-1354/$ – see front matter © 2012 Elsevier Ltd. All rights reserved.
http://dx.doi.org/10.1016/j.watres.2012.06.025

matrices (Cariou et al., 2005), water (de Wit, 2002), air and dust (Abdallah et al., 2008). Previous studies have confirmed that TBBPA is a toxic and persistent compound which can be an endocrine disruptor and seriously affect the development of brain, bone and thyroid hormone systems after a long-term exposure (Birnbaum and Staskal, 2004). Therefore, it is necessary and significant to develop effective techniques to remove TBBPA from the contaminated environment.

In the last decades, several biological and non-biological techniques have been applied in TBBPA degradation. In both aerobic and anaerobic conditions, TBBPA can be degraded by microorganisms with a mean half-life of about two months, suggesting the arduousness of TBBPA degradation by biological methods (Ronen and Abeliovich, 2000). Comparatively, non-biological approaches can achieve a higher degradation rate. Thermal treatment is a traditional method for TBBPA decomposition (Barontini et al., 2004), but it would produce polybrominated debenzo-*p*-dioxins (PBDDs) and dibenzofurans (PBDFs) with higher toxicity during the combustion and pyrolysis processes (Soderstrom and Marklund, 2002). TBBPA also can be oxidized by some transition metal oxides. Lin et al. (2009) revealed that about 50% of TBBPA can be degraded within 5 min by birnessite (δ-MnO_2), but no debromination was observed. In addition, more than 90% of TBBPA was oxidized by a Fe-porphyrin/$KHSO_5$ catalytic system at pH 8.0, and debromination was still not observed (Fukushima et al., 2010). As debromination is a vital step to decrease TBBPA toxicity (Ronen and Abeliovich, 2000), it can be seen that the above non-biological methods were not so effective or environmental friendly. In contrast, photolytic degradation has been considered as a promising technique for TBBPA degradation, due to its capability of achieving debromination and prevalence in the atmosphere and water medium (Chignell et al., 2008). Horikoshi et al. (2008) reported that TBBPA at the concentration of 0.1 mmol L^{-1} could be completely debrominated and degraded by alkaline TiO_2 under 120 min UV radiation, but no discussion on the reaction mechanism was presented in their publication. Nevertheless, knowledge regarding the photo degradation of TBBPA is still rather limited, especially in aspects of degradation pathways and mechanism (Han et al., 2008), which no doubt hinders the application of photolytic degradation in TBBPA removal.

Recently, the heterogeneous Fenton reaction was found available for TBBPA degradation. Luo et al. (2011) revealed that TBBPA was completely degraded in Fenton-like oxidation catalyzed by synthetic Fe–Ag bimetallic nanoparticles under ultrasound radiation. But this kind of prepared catalysts was self-designed and hardly found in the nature, which certainly was uneconomic for its application due to the great consumption wasted during its synthetization. By contrast, with strong catalytic activity, excellent environmental compatibility and universality on the earth surface, magnetite has been considered as an ideal catalyst in heterogeneous Fenton reaction (Ngomsik et al., 2005; Yang et al., 2009a). Our recent studies demonstrated that some magnetite group minerals (e.g. titanomagnetite and V–Ti incorporated magnetite) are effective in degradation of organic dyestuff through heterogeneous Fenton reaction (Liang et al., 2010a; Yang et al., 2009b). Moreover, the introduction of ultraviolet light into Fenton system can obviously improve the pollutant degradation (Muruganandham and Swaminathan, 2004), which has been extensively used in environmental engineering (Wang et al., 2003). However, to the best of our knowledge, there is no report on the degradation of TBBPA through heterogeneous Fenton or UV/Fenton reaction catalyzed by magnetite group minerals (e.g. titanomagnetite).

Hence, in the present study, the degradation of TBBPA through heterogeneous UV/Fenton reaction catalyzed by synthetic titanomagnetite was investigated, with emphasis on the catalytic activity of titanomagnetite, mechanism of titanomagnetite catalyzing TBBPA degradation, degradation pathway of TBBPA, and catalyst reusability. Ultraviolet light was introduced to improve the bioavailability of the degradation system. Therefore, this study is of great significance for developing the application of magnetite group minerals in the UV/Fenton reaction for TBBPA degradation and helpful for us to well understand the environmental fate of TBBPA in the nature.

2. Materials and methods

2.1. Preparation of magnetite samples

Tetrabromobisphenol A (97%) was purchased from Alfa Aesar. Bisphenol A (99%) was obtained from Sigma–Aldrich. Methanol and hexane in ACS certified grade were obtained from Merck while Toluene also in ACS certified grade was provided by Honeywell Burdick & Jackson. The other chemicals and reagents were of analytical grade and used as received.

Fe_3O_4 and titanomagnetite samples ($Fe_{3-x}Ti_xO_4$, $0 \le x \le 1.0$) were prepared by a precipitation–oxidation method and its preparation procedure has been described in detail in the literatures (Liang et al., 2010b; Yang et al., 2009a). All the magnetite samples were ground and passed through a 200-mesh sieve.

2.2. Characterization of magnetite samples

The contents of Fe and Ti in the synthetic samples were analyzed on Varian Vista ICP-AES (Inductively Coupled Plasma Atomic Emission Spectroscopy). Based on the chemical analysis results, the chemical formulae of synthetic magnetite samples were labeled as Fe_3O_4, $Fe_{2.80}Ti_{0.20}O_4$, $Fe_{2.54}Ti_{0.46}O_4$, $Fe_{2.29}Ti_{0.71}O_4$ and $Fe_{2.02}Ti_{0.98}O_4$, respectively. The synthetic samples were characterized by powder X-ray diffraction (PXRD), BET specific surface area, transmission electron microscope (TEM) and X-ray absorption near-edge structure (XANES) spectra. The characterization details are provided in Text A.1 in Supplementary material.

2.3. Heterogeneous UV/Fenton degradation

TBBPA degradation through heterogeneous UV/Fenton reaction was carried out in a home-made photo-reactor with a 6 W UV-light tube ($\lambda = 365$ nm). The mixture of water and methanol (3:2, v/v) was used as solvent to increase the solubility of TBBPA in water. Our preliminary study has confirmed that methanol has no obvious inhibiting or facilitating effect on the degradation process. The 20 mg L^{-1} of TBBPA was used to

simulate the wastewater containing high concentration of TBBPA. After adding titanomagnetite (0.5 g L^{-1}) into the TBBPA solution, the suspension was stirred for 60 min in dark to make the particles and TBBPA well dispersed and achieve the adsorption equilibrium for TBBPA on the catalyst. The degradation was initiated by simultaneously adding H_2O_2 and turning on the UV-light. At given intervals, the reaction solution was sampled for TBBPA concentration analysis and intermediate products identification. The detailed experimental procedures are complementarily provided in Text A.2.

The TBBPA concentration was analyzed by a Shimadzu LC-20A High Performance Liquid Chromatography (HPLC), and the degradation intermediate products were identified by a Shimazu QP2010 plus Gas Chromatographic Mass Spectrometry (GC-MS). The leaching Fe ions concentration during degradation was analyzed on a PE-3100 Flame Atomic Absorption Spectrophotometer (FAAS). The detailed instrument conditions are shown in Text A.3. In addition, the solid catalyst was recycled after degradation and ready for XRD and XANES characterizations and reusability test.

To investigate the contribution of homogeneous UV/Fenton process catalyzed by the leaching Fe ions on the TBBPA degradation, experiments in two homogeneous systems UV/$FeSO_4/H_2O_2$ and UV/$Fe_2(SO_4)_3/H_2O_2$ were also carried out. Additional experiment details are described in Text A.2.

3. Results and discussion

3.1. Characterization of magnetite samples

Fig. 1 shows that the XRD patterns of the synthetic samples well correspond to the standard card of magnetite (JCPDS: 19-0629), indicating that the synthetic samples have well crystallized spinel structure. Table 1 displays the lattice parameter (a_0), BET surface area and particle size of $Fe_{3-x}Ti_xO_4$. The lattice parameter a_0 of all the titanomagnetite samples is

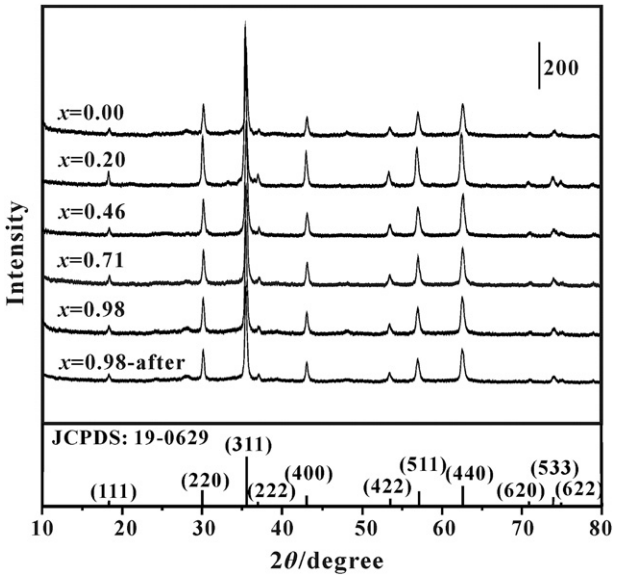

Fig. 1 – X-ray diffraction patterns of the synthetic $Fe_{3-x}Ti_xO_4$ ($0 \le x \le 1.0$) samples.

Table 1 – Lattice parameters, BET surface areas and particle sizes of the $Fe_{3-x}Ti_xO_4$.

Sample	a_0/m	Surface area /m^2 g^{-1}	Average particle size/nm	Particle size distribution/nm
Fe_3O_4	0.8392	19	82	34–245
$Fe_{2.80}Ti_{0.20}O_4$	0.8371	38	67	36–164
$Fe_{2.54}Ti_{0.46}O_4$	0.8362	50	58	25–118
$Fe_{2.29}Ti_{0.71}O_4$	0.8364	58	56	27–94
$Fe_{2.02}Ti_{0.98}O_4$	0.8365	57	55	31–85

smaller than that of Fe_3O_4. Moreover, with the increase of titanium incorporation, the specific surface area gradually increases while the particle size decreases.

The TEM images of the catalyst samples are shown in Fig. 2. Fe_3O_4 grows well in an octahedral shape which is the classical morphology of well crystallized magnetite. And more than 90% of particles are in size of 30–200 nm with the average size at 82 nm. With the increase of titanium content, the average particle size decreases and the size distribution becomes narrow (Table 1).

The catalytic activity of transition metal substituted magnetite is strongly dependent on the nature of substituting cations, the valences and distribution over the tetrahedral and octahedral sites (Lee et al., 2008). Herein, XANES characterization was carried out to probe the valence and occupancy of titanium in the synthetic titanomagnetite samples. From previous study (Simon et al., 2007), the intensity and energy position of the pre-edge peak are quite sensitive to the valence of absorbing atoms, which also is a fingerprint to distinguish tetrahedral coordination from octahedral one. The left panel of Fig. 3 displays the normalized Ti K-edge XANES spectra of $Fe_{3-x}Ti_xO_4$ and Ti reference compounds. The pre-edge curves for both rutile (α-TiO_2) and anatase (γ-TiO_2) show three peaks (respectively labeled as A, B, and C in the right panel of Fig. 3). The curve profiles for both rutile and anatase are quite different from that of Ti foil. The perturbation A, related to the shake up and shake off process, derives from an exciton band or a transition from 1s to $1t_{1g}$. And perturbations B and C are originated from the transitions from 1s to $2t_{2g}$ and from 1s to $3e_g$ in an octahedral field, respectively (Liu et al., 2003a; Pickup et al., 2008). From previous studies, the intensity variation of these three pre-edge peaks is mainly related to the changes in the distortion of the octahedral TiO_6 unit (Liu et al., 2003a; Simon et al., 2007). And peak B should become more intense and shift to lower energy when the coordination of titanium changes from sixfold to fourfold. Moreover, peak C is quite sensitive to the distortion degree, ascribed to the energy minimization of structure. Its intensity increases with the increase of distortion degree around the absorbing atom site (Pickup et al., 2008). For titanomagnetite, the intensity of pre-edge peaks increases with the increase of titanium content. Especially for perturbation B, this peak on the curve of $Fe_{2.02}Ti_{0.98}O_4$ is more intensive than that of $Fe_{2.97}Ti_{0.03}O_4$. But the pre-edge feature of all the titanomagnetite samples is still in low intensity. Moreover, from the left panel of Fig. 3, it is obvious that intensity and position of the absorption edge for $Fe_{3-x}Ti_xO_4$ are respectively identical to those of ilmenite

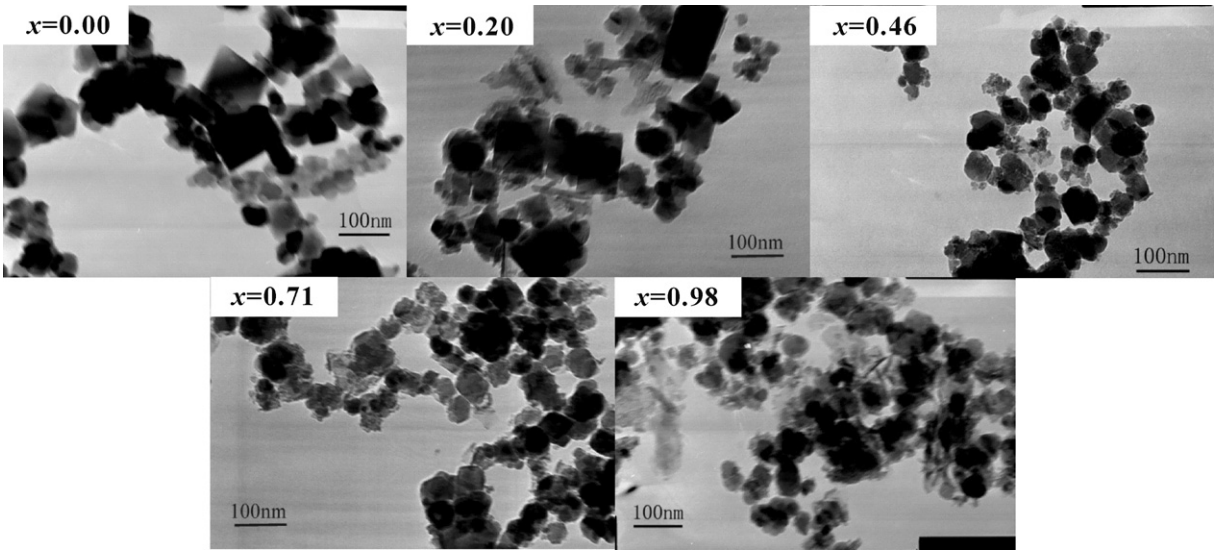

Fig. 2 – TEM images of the synthetic $Fe_{3-x}Ti_xO_4$ ($0 \le x \le 1.0$) samples.

($FeTiO_3$) with octahedral Ti^{4+}. This indicates that titanium cations in titanomagnetite have the valence of +4 and limit to the octahedral sites, which are consistent with results of the previous studies (Pearce et al., 2010; Wechsler et al., 1984). Furthermore, the low intensity of peak C suggests the low distortion degree around the titanium cations, ascribed to the small difference in ionic radius between Ti^{4+} (60.5 pm) and Fe^{3+} (65 pm) in octahedral sites (Gasmi et al., 2009; Liu et al., 2003b). This is in accordance with the slight decrease in lattice parameter a_0 (Table 1).

In titanomagnetite, the valences of iron are +3 and +2 (Yang et al., 2009a). Based on the principle of electrovalence equilibrium (Pearce et al., 2010), when Ti^{4+} substituted partial Fe^{3+} in magnetite structure, same amount of Fe^{3+} would be changed to Fe^{2+}. But when Ti^{4+} substituted Fe^{3+} without Fe^{2+} generation, the electrovalence equilibrium was balanced by producing oxygen vacancy and structural defect compensation (Liu et al., 2008; Moura et al., 2006).

3.2. TBBPA degradation in different catalytic systems

To investigate the catalytic activity of titanomagnetite for the UV/Fenton degradation of TBBPA, series of contrast experiments were carried out. As shown in Fig. 4, the concentration of TBBPA did not obviously decrease in the presence of $Fe_{2.02}Ti_{0.98}O_4$ alone. It indicated that TBBPA was hardly adsorbed on the titanomagnetite surface, because the removal of TBBPA in $Fe_{2.0}Ti_{0.98}O_4$ system mainly depended on the adsorption on $Fe_{2.02}Ti_{0.98}O_4$. The low adsorption may be ascribed to the fact that TBBPA was a hydrophobic compound while titanomagnetite surface was hydrophilic. Similarly, no significant decrease in the TBBPA concentration was observed in the $Fe_{2.02}Ti_{0.98}O_4/H_2O_2$ system. It may be attributed to the slow reaction between $\equiv Fe^{II}$ on magnetite surface and H_2O_2 under near neutral pH condition, and the insufficient $^{\bullet}OH$ radical generation. The high generation rate of $^{\bullet}OH$ radicals shown in Eq. (1) was obtained only under acid pH condition

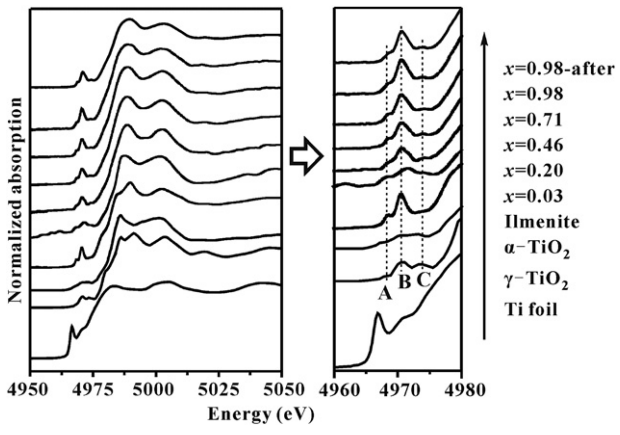

Fig. 3 – XANES spectra of $Fe_{3-x}Ti_xO_4$ ($0 < x \le 1.0$) and Ti reference compounds.

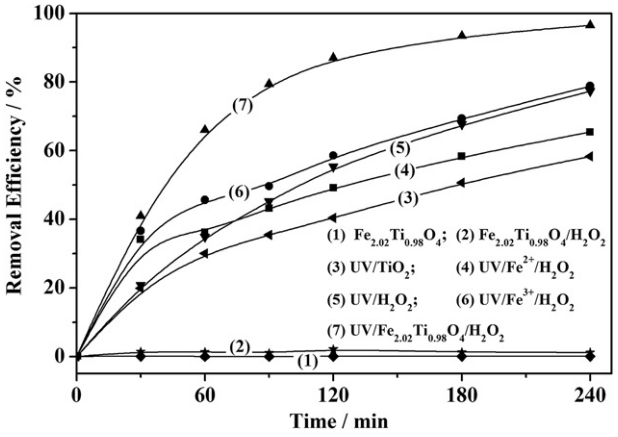

Fig. 4 – TBBPA degradation in different systems (TBBPA: 20 mg L^{-1}, H_2O_2: 10 mmol L^{-1}, $Fe_{2.02}Ti_{0.98}O_4$: 0.50 g L^{-1}, Fe^{3+}: 20 mg L^{-1}, 500 mL, pH: 6.5, 25 °C).

(De Laat and Gallard, 1999). Moreover, the insufficient •OH radicals were easily scavenged by H_2O_2 (Eq. (2)) (Perez et al., 2002), so the generated •OH were not enough to diffuse into the bulk solution to degrade TBBPA (Kwan and Voelker, 2002). Besides, the low TBBPA adsorption on magnetite surface also led to its difficult degradation.

$$\equiv Fe^{II} + H_2O_2 \rightarrow \equiv Fe^{III} + {}^{\bullet}OH + OH^-,\ k_1 = 63\ M^{-1}\ s^{-1} \quad (1)$$

$$^{\bullet}OH + H_2O_2 \rightarrow HO_2^{\bullet} + H_2O,\ k_2 = 2.7 \times 10^7\ M^{-1}\ s^{-1} \quad (2)$$

Compared to $Fe_{2.02}Ti_{0.98}O_4/H_2O_2$ system, UV/H_2O_2 system showed more effective in the degradation of TBBPA. Approximately 75% of TBBPA was degraded after 240 min UV irradiation in UV/H_2O_2 system. The degradation of TBBPA by UV/H_2O_2 was attributed to the attack of •OH radicals generated by photolysis of H_2O_2 as shown in Eq. (3) (Chen and Zhu, 2007). Previous studies have also reported the higher efficiency of UV/H_2O_2 system than heterogeneous Fenton system in the degradation of other organic pollutants (Anipsitakis and Dionysiou, 2004; Zhang et al., 2007).

$$H_2O_2 + h\upsilon \rightarrow 2^{\bullet}OH \quad (3)$$

When titanomagnetite ($Fe_{2.02}Ti_{0.98}O_4$) was introduced to the UV/H_2O_2 system, the degradation efficiency of TBBPA was significantly enhanced. More than 97% of TBBPA was degraded after 240 min UV irradiation. Such enhancement was attributed to the fact that the generated Fe^{III} (Eq. (1)) on the titanomagnetite surface under UV irradiation (365 nm) could be effectively reduced to Fe^{II} with concomitant production of •OH radicals (Eq. (4)) (Tryba et al., 2009; Utset et al., 2000). The regenerated Fe^{II} can further participate in the Fenton reaction to produce •OH radicals (Eq. (1)). Such recycle enhanced the •OH radical production and made the UV/Fenton system display efficient catalytic activity for the degradation of TBBPA.

$$\equiv Fe^{III} + H_2O_2 + h\upsilon \rightarrow \equiv Fe^{II} + 2^{\bullet}OH \quad (4)$$

Compared to the UV/$Fe_{2.02}Ti_{0.98}O_4/H_2O_2$ system and UV/H_2O_2 system, the UV/TiO_2 system exhibited weaker catalytic activity towards the degradation of TBBPA, and only about 58% of degradation was obtained after 240 min UV radiation.

To investigate the possibility that the observed catalytic activity of titanomagnetite was caused by the Fe leaching from the catalyst, the concentrations of Fe ions in the solution of UV/$Fe_{2.02}Ti_{0.98}O_4/H_2O_2$ system was tracked (Fig. A.1). It was observed that the concentration of dissolved Fe ions was proportional to the reaction time (left panel of Fig. A.1), and a logarithm relationship between the dissolved Fe ions concentration and magnetite dosage can be seen in the right panel of Fig. A.1. Furthermore, the concentrations of dissolved Fe ions in reaction solutions increased from 3 to 20 mg L^{-1} as the catalyst dosage increased from 0.125 to 1.0 g L^{-1} after 240 min reaction.

Owing to the obvious Fe leaching from catalyst in this study, it was not clear whether the homogeneous UV/Fenton reaction was responsible for the fast degradation of TBBPA or not. Therefore, two homogeneous systems of UV/$FeSO_4/H_2O_2$ and UV/$Fe_2(SO_4)_3/H_2O_2$ were performed (Fig. 4). The initial iron concentrations in both systems were chosen at 20 mg L^{-1}, according to the maximum Fe leaching amounts during the UV/Fenton degradation of TBBPA by $Fe_{2.02}Ti_{0.98}O_4$ (right panel of Fig. A.1). As shown in Fig. 4, in the UV/$Fe_2(SO_4)_3/H_2O_2$ system, around 78% of TBBPA was degraded after 240 min reaction, which was comparable to that of UV/H_2O_2 system without titanomagnetite (77%), suggesting that the contribution of dissolved Fe^{3+} ions to the TBBPA degradation in UV/H_2O_2 system was negligible. It may be due to the fact that Fe^{3+} reacted slowly with H_2O_2 to generate $HO_2^{\bullet}$ radicals with lower activity than •OH radicals (Eq. (5)). However, the lower degradation percentage of TBBPA (66%) was obtained in the UV/$FeSO_4/H_2O_2$ system (77%). The lower efficiency of this homogeneous UV/Fenton system was probably related to the fact that the titrimetric addition of H_2O_2 in our study may result in locally high concentration of H_2O_2, which could induce the •OH radical scavenging effect (De Laat and Gallard, 1999; Zepp et al., 1992). Especially, the highly oxidative •OH radicals generated from the fast reaction between Fe^{2+} and H_2O_2 (Eq. (6)) could quickly react with H_2O_2 to form the weaker oxidative $HO_2^{\bullet}$ radicals Eq. (2), leading to the slow degradation of TBBPA. It should be noted that the scavenging effect would be negligible in UV/$Fe_2(SO_4)_3/H_2O_2$ system, since the reactivity of Fe^{3+} with H_2O_2 was very low (Eq. (5)), thus less radicals could be scavenged by H_2O_2.

$$Fe^{3+} + H_2O_2 \rightarrow Fe^{2+} + HO_2^{\bullet} + H^+,\ k_3 = 0.02\ M^{-1}\ s^{-1} \quad (5)$$

$$Fe^{2+} + H_2O_2 \rightarrow Fe^{3+} + {}^{\bullet}OH + OH^-,\ k_4 = 58\ M^{-1}\ s^{-1} \quad (6)$$

These results indicated that the contribution of the homogeneous UV/Fenton reaction catalyzed by dissolved Fe ions at near neutral pH can be ignored. The fast degradation of TBBPA was mainly dominated by the heterogeneous UV/Fenton reaction catalyzed by titanomagnetite.

Under these tested conditions, all the degradation processes were well fitted with the pseudo-first-order rate kinetic law (Eq. (7)) (Liang et al., 2010b), with correlation coefficients higher than 0.95 (Fig. A.2).

$$-\ln(C_t/C_0) = k_{app}t \quad (7)$$

where C_0 and C_t are the TBBPA concentrations at the initial time and reaction time t, respectively, mg L^{-1}, k_{app} is the apparent pseudo-first-order rate constant, min^{-1}.

The obtained k_{app} were 0.015, 0.0063, 0.0058, 0.0039, 0.0034, 1.8×10^{-4} and 9.2×10^{-5} min^{-1} for the systems of UV/$Fe_{2.02}Ti_{0.98}O_4/H_2O_2$, UV/$H_2O_2$, UV/$Fe_2(SO_4)_3/H_2O_2$, UV/$FeSO_4/H_2O_2$, UV/$TiO_2$, $Fe_{2.02}Ti_{0.98}O_4/H_2O_2$ and $Fe_{2.02}Ti_{0.98}O_4$, respectively. The catalytic activity on the degradation of TBBPA in the above systems obeys the following order: UV/$Fe_{2.02}Ti_{0.98}O_4/H_2O_2$ > UV/H_2O_2 > UV/TiO_2 > $Fe_{2.02}Ti_{0.98}O_4/H_2O_2$ > $Fe_{2.02}Ti_{0.98}O_4$. TBBPA could not be degraded efficiently in the $Fe_{2.02}Ti_{0.98}O_4/H_2O_2$ system, while the introduction of UV

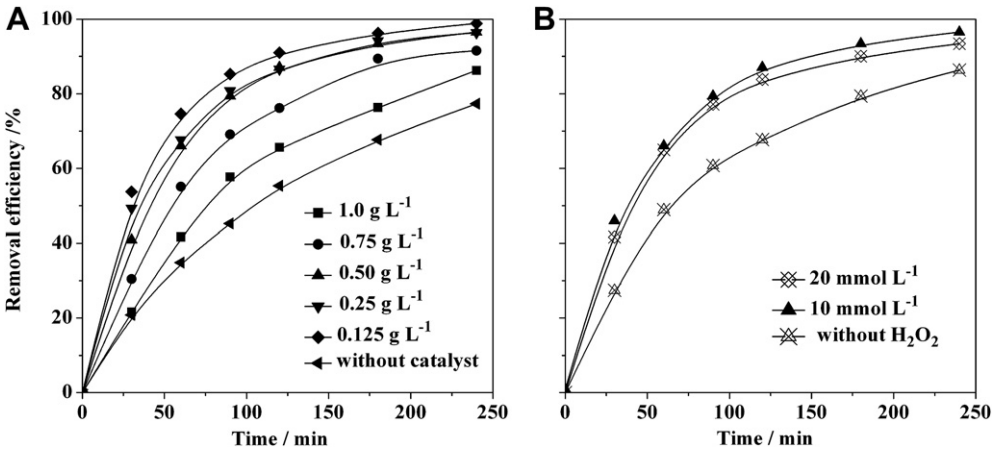

Fig. 5 – Effect of $Fe_{2.02}Ti_{0.98}O_4$ loading (A) and H_2O_2 dosage (B) on the degradation of TBBPA (C_0 = 20 mg l^{-1}, H_2O_2 (A), 10 mmol L^{-1}; catalyst (B), 0.50 g L^{-1}, 500 mL, pH = 6.5, 25 °C).

greatly improved its degradation. As titanomagnetite was a common mineral with great reserve, the combination of UV and Fenton process should be an efficient and economic technology.

3.3. *Parameters for UV/Fenton degradation of TBBPA catalyzed by titanomagnetite*

3.3.1. *Effect of titanomagnetite dosage*

The effect of titanomagnetite ($Fe_{2.02}Ti_{0.98}O_4$) dosage ranging from 0 to 1.0 g L^{-1} on TBBPA degradation was investigated under the optimal reaction conditions (pH 6.5, 10 mmol L^{-1} H_2O_2, 20 mg L^{-1} TBBPA, and 240 min UV irradiation). As shown in Fig. 5A, TBBPA degradation percentage increased from 77% to 99% when titanomagnetite dosage was increased from 0 to 0.125 g L^{-1}, indicating the highly catalytic activity of titanomagnetite in the TBBPA degradation. However, with the catalyst dosage up to 1.0 g L^{-1}, the TBBPA degradation efficiency decreased by 86%. The decline in the degradation of TBBPA may be ascribed to the fact that the turbidity of suspension in the presence of excessive catalyst would decrease the penetration of UV-light, resulting in a loss of available radiation via light scattering (Vicente et al., 2009). Consequently, the generation of effective photons was decreased and then the photo-catalytic activity was reduced (Bangun and Adesina, 1998). Furthermore, previous studies have reported that the excessive catalysts were hydroxyl radical scavengers (Eq. (8)), and hence reduced the amounts of generated •OH radicals in the system (Malik, 2004; Neyens and Baeyens, 2003).

$$Fe^{2+} + {}^{\bullet}OH \leftrightarrow Fe^{3+} + OH^{-} \quad (8)$$

3.3.2. *Effect of H_2O_2 concentration*

The effect of H_2O_2 concentration ranging from 0 to 20 mmol L^{-1} on the TBBPA degradation in the presence of titanomagnetite ($Fe_{2.02}Ti_{0.98}O_4$) and UV irradiation was studied. Compared to control system in the absence of H_2O_2, the addition of 10 mmol L^{-1} H_2O_2 resulted in an increase in degradation of TBBPA (Fig. 5B). It may be attributed to that H_2O_2 can inhibit the recombination of electron–hole pair and its photolysis can produce •OH radicals for TBBPA degradation (Eqs. (3) and (9)) (Chong et al., 2010). However, with the H_2O_2 concentration up to 20 mmol L^{-1}, the degradation efficiency of TBBPA significantly decreased. This phenomenon can be explained by the fact that excess H_2O_2 can react with •OH radicals to form $HO_2^{\bullet}$ radicals (Eq. (2)). As mentioned above, the oxidation potential of $HO_2^{\bullet}$ radicals is much lower than that of •OH radicals (Chong et al., 2010; Daneshvar et al., 2003; Ramirez et al., 2007), and it can react with •OH radicals and consequently decrease the degradation efficiency of TBBPA (Chen et al., 2010).

$$H_2O_2 + e^{-} \rightarrow {}^{\bullet}OH + HO^{-} \quad (9)$$

3.3.3. *Effect of titanium incorporation*

The UV/Fenton degradation of TBBPA catalyzed by synthetic titanomagnetite with different titanium contents was shown in Fig. 6. Under the tested conditions, all the degradation processes were well fitted with the pseudo-first-order rate kinetic law (Eq. (7)), with correlation coefficients higher than 0.95. The obtained k_{app} for UV/H_2O_2 and UV/Fenton systems catalyzed by Fe_3O_4, $Fe_{2.80}Ti_{0.20}O_4$, $Fe_{2.54}Ti_{0.46}O_4$, $Fe_{2.29}Ti_{0.71}O_4$ and $Fe_{2.02}Ti_{0.98}O_4$ is 0.0061, 0.0065, 0.0084, 0.0070, 0.0011 and 0.015 min^{-1}, respectively. It was observed that k_{app} basically increased with the increase of titanium content in magnetite, suggesting that titanium incorporation played an important role in strengthening the catalytic activity of magnetite in UV/Fenton reaction. There are two possible reasons for this positive effect. One is that the isomorphism substitution of Ti^{4+} for Fe^{3+} in magnetite could create some defects and dislocations in magnetite structure due to their unequal valence, resulting in the formation of oxygen vacancies and Fe^{3+} reduction to Fe^{2+} to keep electrovalent equilibrium (Pearce et al., 2010). The other one is that Ti^{4+} on the titanomagnetite surface can be reduced to Ti^{3+} under the UV irradiation and oxygen vacancies were simultaneity produced (Eq. (10)) (Anpo et al., 1999; Liu et al., 2003a).

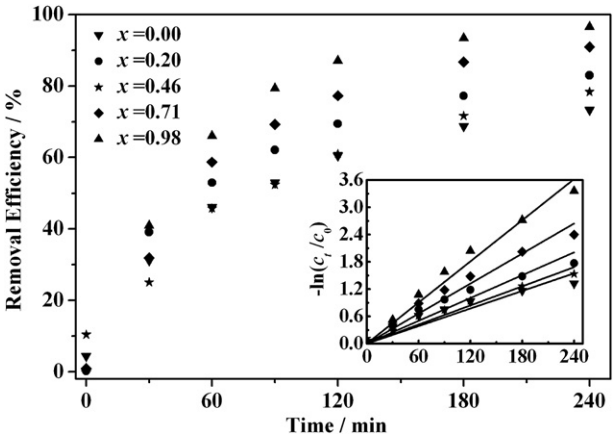

Fig. 6 – The kinetics process of TBBPA degradation in UV/Fenton reaction catalyzed by $Fe_{3-x}Ti_xO_4$ ($0 \le x \le 1.0$). Inset: The kinetics process fitted by pseudo-first-order rate law (TBBPA: 20 mg L^{-1}, H_2O_2: 10 mmol L^{-1}, catalyst: 0.50 g L^{-1}; 500 mL, pH: 6.5, 25 °C).

$$2Ti^{4+} + O^{2-} + h\upsilon \rightarrow 2Ti^{3+} + (1/2)O_2 + AV \quad (10)$$

where AV is anion vacancy.

It is known that these oxygen vacancies and defects are the active sites for the generation of •OH radicals and the regeneration of Fe^{2+} which can further accelerate the Fenton degradation reaction (Jing et al., 2004; Li et al., 2005a,b). Therefore, titanium substitution in magnetite was able to promote the TBBPA degradation by enhancing the reduction of Fe^{3+} to Fe^{2+} and the generation of •OH radicals.

Nevertheless, there was an unexpected decline in catalytic efficiency for $Fe_{2.54}Ti_{0.46}O_4$, while compared with $Fe_{2.80}Ti_{0.20}O_4$ (Fig. 6). This phenomenon is probably related to the substitution extent of Fe^{3+} by Ti^{4+} in the octahedral sites. It has been established that the catalytic activity is mainly dependent on the octahedral cations, as the octahedral sites are almost exclusively exposed at the surface of the spinel structure (Ramankutty et al., 2002). As an inverse spinel mineral, magnetite has the structure of $Fe^{3+}{}_{tet}(Fe^{2+}, Fe^{3+})_{oct}O_4$. As mentioned above, when Ti^{4+} substitutes partial Fe^{3+} in magnetite structure, the same amount of Fe^{3+} is changed to Fe^{2+} to keep electrovalence equilibrium. Furthermore, for $Fe_{3-x}Ti_xO_4$, when the substitution extent x was below 0.50, the electron transfer promoted by UV irradiation predominately between Fe^{2+} and Fe^{3+} in octahedral sites (Pearce et al., 2010). Herein, the electron transfer between Fe^{2+} and Fe^{3+} mainly occurs on face-shared and edge-shared octahedral. But when the substitution extent x is close to 0.5, nearly all the Fe^{3+} in octahedral sites are substituted by Ti^{4+} or changes to Fe^{2+} and no octahedral sites are occupied by Fe^{3+} (Pearce et al., 2010), which could greatly weaken the electron transfer between Fe^{2+} and Fe^{3+} on edge-shared octahedral sites. Although the more Ti^{4+} can generate more oxygen vacancies, it is possibly insufficient to cover the weakening effect of the electron transfer, resulting in the slightly weaker catalytic activity of $Fe_{2.54}Ti_{0.46}O_4$ than that of $Fe_{2.80}Ti_{0.20}O_4$.

While the substitution extent x was higher than 0.5, Ti in octahedral sites can efficiently block the electron transfer between Fe^{2+} and Fe^{3+} and the intervalence transition between Fe^{2+} and Ti^{4+} dominates (Eq. (11)) (Burns, 1981; Seda and Hearne, 2004). Both of them may contribute to the gradual increase in catalytic activity of titanomagnetite for substitution extent higher than 0.5.

$$Ti^{4+} + Fe^{2+} \rightarrow Ti^{3+} + Fe^{3+} \quad (11)$$

3.4. *Identification of products and reaction mechanism in methanol/water*

There were twelve degradation products of TBBPA identified by GC-MS, assigned as Products **1**–**12**, respectively. Except Product **5**, the other products were tentatively identified by comparing with identified products from the degradation of TBBPA reported in published literatures due to the lack of authentic standards. In addition, the mass spectrum of TBBPA was used as reference to interpret the fragmentation pattern of products. Table 2 exhibits the mass spectra data of all products, including the molecular structures and characteristic fragment ions. The Products **1**–**4** were identified as tribromobisphenol A (TriBBPA), dibromobisphenol A (DiBBPA, two isomers), and monobromobisphenol A (MonoBBPA), respectively, by comparing their mass spectra with those of products from the transformation of TBBPA identified in literatures (Barontini et al., 2004; Blazso et al., 2002). Product **5** was identified as bisphenol A (BPA) by the authentic standards. Product **6** was tentatively identified as phenol, since it had the identical mass spectrum to that of phenol reported by Borojovich and Aizenshtat (2002) and Hornung et al. (2003), with a molecular ion (M^+) at m/z 94 [100, M^+] (relative intensity, %, and formula of assigned ion fragment) and fragment ion at m/z 77 [15.2, $(M - OH)^+$]. Products **7**–**10** were tentatively identified as 4-isopropylene-2,6-dibromophenol (**7**), 4-(2-hydroxyisopropyl)-2,6-dibromophenol (**8**), 4-isopropyl-2,6-dibromophenol (**9**), and 2-(2,4-cyclopentadienyl)-2-(3,5-dibromo-4-hydroxyphenyl) propane (**10**), respectively, by comparison with published mass spectra data (Barontini et al., 2004; Eriksson et al., 2004; Hornung et al., 2003; Lin et al., 2009). The identification of above Products **1**–**10** has been described in detail in Text A.4 of the Supplementary material. In addition, Products **11** and **12** had the same molecular weight (m/z 430) and similar fragmentation pattern (shown in Text A.4) but with different retention times, suggesting that they might be isomers. According to the analysis of their mass spectra (Fig. A.3), they were tentatively identified as dibromo-4-[2-(4-hydroxy phenyl)] isopropoxy benzoic acid. Due to lack of authentic standards, their substituent position of bromines was uncertain.

On the basis of the identified products, the degradation pathways of TBBPA under heterogeneous UV/Fenton process were proposed (shown in Fig. 7). It is well accepted that the heterogeneous UV/Fenton process is based on the reaction of •OH radicals which can destroy organic pollutants efficiently (Litter, 1999). As shown in Fig. 7, the proposed reaction mechanisms for the degradation of TBBPA involved two different pathways (Schemes 1 and 2), corresponding to the

Table 2 – Mass spectra data of intermediate products.

Product	Retention time (min)	Molecular weight	Fragmentation ions	Proposed Structure
1	27.64	465	450, 370, 291, 210	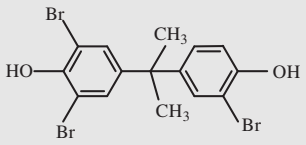
2	23.03	386	371, 291, 211	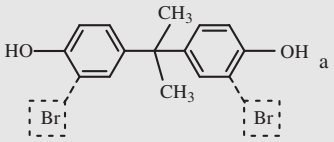 a
3	26.05	386	371, 290, 211	
4	21.24	308	293, 278, 212, 197	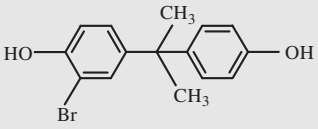
5	10.59	228	211, 196, 181, 105	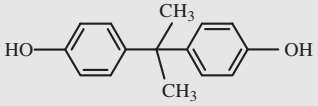
6	8.04	94	77	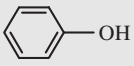
7	9.66	292	277, 212, 196, 132	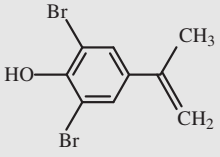
8	11.62	310	293, 212, 132, 91	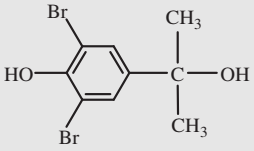
9	12.21	294	279, 214, 199, 184, 104	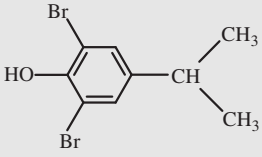
10	17.90	358	343, 293, 262, 198, 183	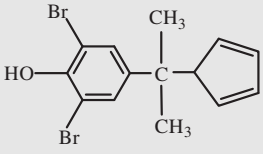
11	26.17	430	416, 401, 385, 335, 320, 275, 212, 133	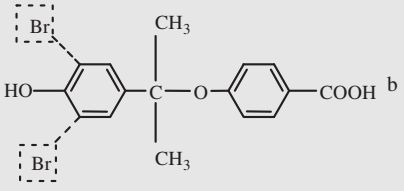 b
12	26.48	430	416, 401, 356, 339, 320, 275, 241, 196	

a Products **2** and **3** are isomers.
b Products **11** and **12** are isomers. The uncertain substituent positions of bromines are displayed in dotted boxes.

two possible sites for the attack of •OH radicals on the TBBPA molecule. In Scheme 1, the generated •OH radicals may attack the C–Br bond of TBBPA and lead to debromination of TBBPA to form TriBBPA, DiBBPA, MonoBBPA and BPA. The sequential debromination pathway of TBBPA often occurred in the reductive degradation of TBPPA by anaerobic bacteria and zero-valent metals (Barontini et al., 2004; Blazso et al., 2002; Ronen and Abeliovich, 2000). Although Eriksson et al. (2004) had found the photochemical degradation of TBBPA via Tri-, di- and monoBBPA as well as BPA were not detected. Xu et al. (2011) have investigated TBBPA degradation by BiOBr under simulated light irradiation and reported that the debromination of TBBPA was concomitant with hydroxylation to yield tetrahydroxylated BPA. Horikoshi et al. (2008) have found the

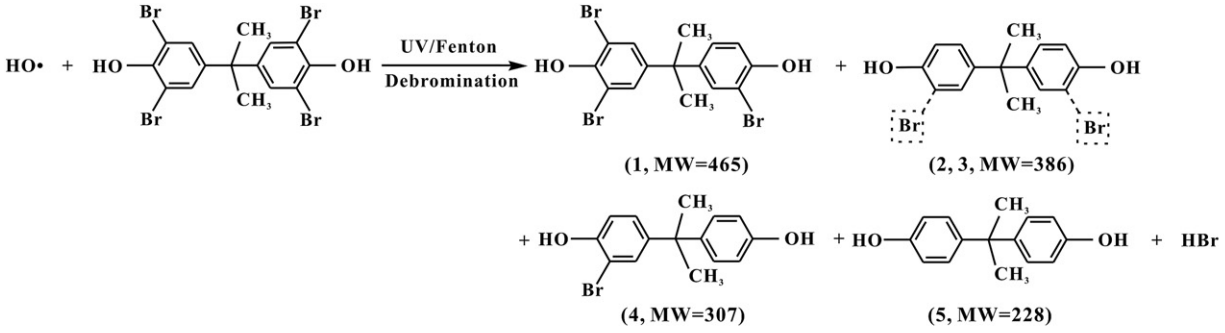

Scheme 1: Debromination processes

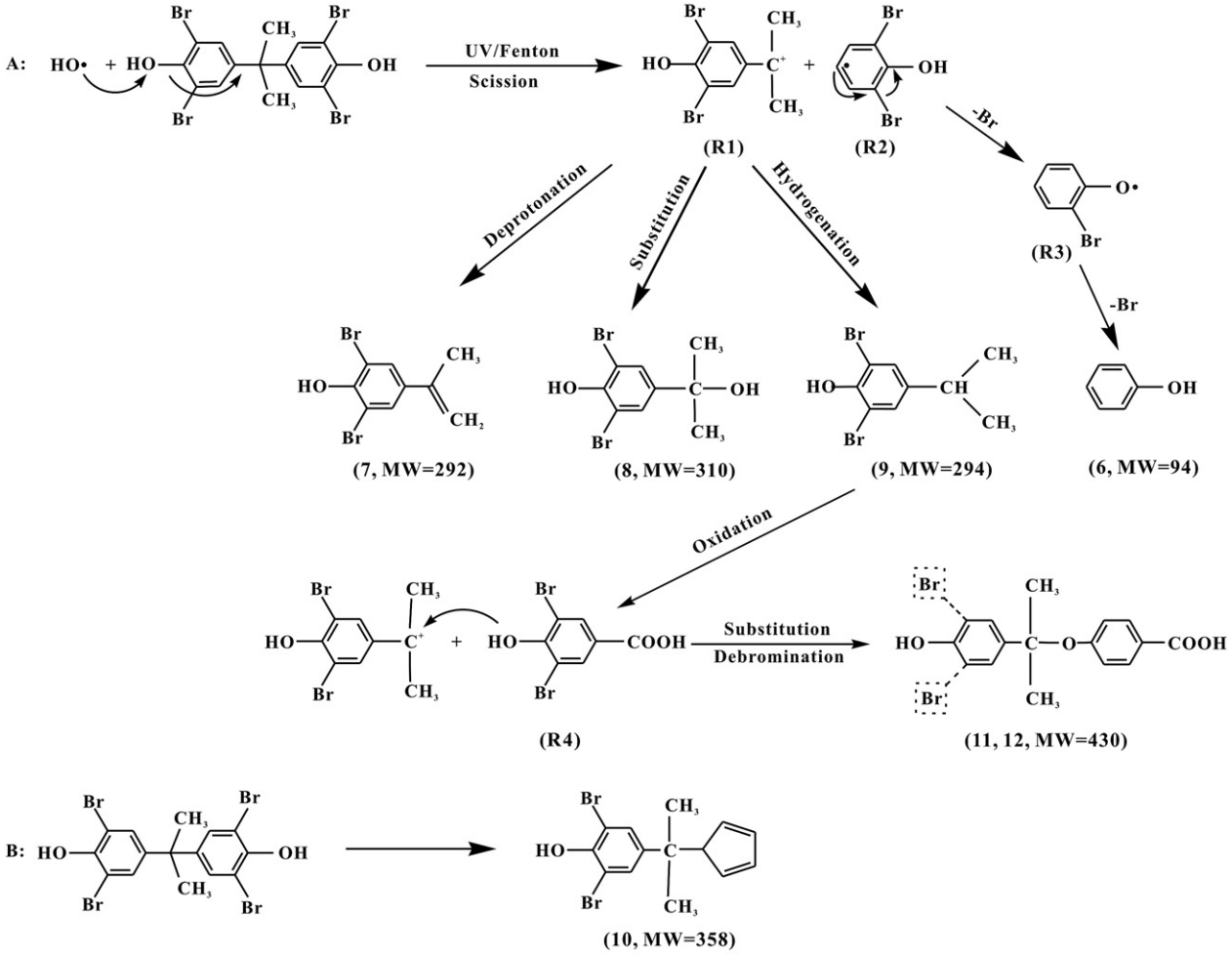

Scheme 2: Decomposition and transformation processes

Fig. 7 – Proposed reaction schemes for TBBPA degradation in UV/Fenton reaction (The uncertain substituent position of bromines was displayed in dotted boxes).

formation of bromine ions from TBBPA degradation in UV-irradiated alkaline aqueous TiO_2 dispersions, while they did not identify the degradation products of TBBPA and cannot examine the debromination mechanism. To our knowledge, this is the first report of sequential debromination of TBBPA taking place in the heterogeneous UV/Fenton reaction.

In addition to sequential debromination, TBBPA may undergo β-scission (cleavage between one of the benzene rings and the isopropyl group) by oxidation of $^{\bullet}OH$ radicals to yield a cationic intermediate **R1** and a radical **R2** (Scheme 2A). **R1** may be transferred to 4-isopropylene-2,6-dibromophenol (**7**), 4-(2-hydroxyisopropyl)-2,6-dibromophenol (**8**), 4-isopropyl-2,6-dibromophenol (**9**) through deprotonation, substitution and hydrogenation reactions, respectively. This pathway has been extensively reported in the oxidative degradation of TBBPA by $^{\bullet}OH$ radicals, UV-light, and singlet oxygen (Barontini et al., 2004; Eriksson et al., 2004; Lin et al., 2009). Due to $^{\bullet}OH$ radicals are nonselective, they can react directly with intermediates of TBBPA. Radical **R2** may be transformed into phenol (Product **6**) via debromination by the oxidation of $^{\bullet}OH$ radicals. Product **9** contained an active benzyl carbon–hydrogen bond which was easily attacked by $^{\bullet}OH$ radicals (Guo et al., 2003), so it may be further oxidized to form intermediate Product **R4** followed by coupling with **R1** to yield isomeric Products **11** and **12** (Scheme 2A). Product **10** has been detected in the photodegradation of TBBPA by Eriksson et al. (2004), while its production mechanism has not yet been clearly studied (Scheme 2B) and the further study is needed to uncover the possible mechanism.

The concentrations of these detected products were semiquantitatively determined by comparing their relative peak area response to that of TBBPA. The results showed that after 240 min reaction, the debromination products including TriBBPA, DiBBPA, MonoBBPA and BPA accounted for about 42.5% of the production of products, and there remained 57.5% products probably originated from the β-scission process and its correlative chain reactions. It suggested that both of the debromination and β-scission reaction were the dominant TBBPA degradation pathways in UV/Fenton reaction catalyzed by titanomagnetite. It is worth mentioning that the amounts of all products initially reached a maximum and subsequently decreased to undetected level with the reaction time, suggesting that heterogeneous UV/Fenton reaction catalyzed by titanomagnetite can provide fast and complete degradation of major intermediate products of TBBPA.

3.5. *Reusability of titanomagnetite*

Undoubtedly, reusability is an important factor for the application of catalyst in economic perspective. Fig. A.4 shows the TBBPA degradation in UV/Fenton reaction catalyzed by $Fe_{2.02}Ti_{0.98}O_4$ after three recycles. It can be seen that the reused catalyst $Fe_{2.02}Ti_{0.98}O_4$ still retained the catalytic activity as efficient as the first cycle, and more than 90% TBBPA was degraded in the third run. Although there was some Fe dissolved during the reaction, it did not negatively affect the catalytic activity of titanomagnetite in several cycles. In addition, the analysis of XRD and XANES also confirmed the chemical stability of catalysts $Fe_{2.02}Ti_{0.98}O_4$ during the three recycles (Figs. 1 and 3). It was observed that the spinel structure and titanium coordination environment of the reused catalysts $Fe_{2.02}Ti_{0.98}O$ were almost the same as that of the fresh catalysts after 240 min of reaction (Figs. 1 and 3). These results demonstrated that titanomagnetite as catalyst has good stability and reusability.

Some catalysts with high efficiency in the TBBPA degradation have been reported in literatures, such as Fe-porphyrin/$KHSO_5$ (Fukushima et al., 2010), Fe–Ag bimetallic nanoparticles (Luo et al., 2011), Mesoporous BiOBr microspheres (Xu et al., 2011), while they are often expensive and cannot be reused without loss of catalytic activity. Titanomagnetite, which are ubiquitously present in the environment and readily available, can overcome these drawbacks. Furthermore, titanomagnetite as heterogeneous catalysts exhibited a higher catalytic activity towards the UV/Fenton degradation of TBBPA, compared to the traditional homogeneous Fenton reaction, UV/TiO_2 reaction and UV/H_2O_2 reaction (Fig. 4). Hence, titanomagnetite may be a promising heterogeneous catalyst applied to the removal of TBBPA from wastewater due to its low cost, high efficiency, and high reusability. Furthermore, it may play an important role in the environmental fate of TBBPA, contributing to the abiotic transformation of this pollutant in the presence of naturally occurring H_2O_2 and UV-light.

4. Conclusions

This study demonstrated that the titanomagnetite as heterogeneous catalysts had strong catalytic activity for the UV/Fenton degradation of TBBPA. The effects of experimental parameters (i.e., catalyst dosage, H_2O_2 concentration, and titanium content) on the degradation of TBBPA have been evaluated in batch experiments. The fastest degradation of TBBPA occurred under the optimal conditions with 0.125 g L^{-1} of $Fe_{2.02}Ti_{0.98}O_4$, 10 mmol L^{-1} of H_2O_2 and 240 min UV irradiation. The introduction of Ti^{4+} significantly improved the catalytic activity of magnetite. Based on the identification of products by GC-MS, the degradation pathways of TBBPA were proposed, which mainly involved debromination to form TriBBPA, DiBBPA, MonoBBPA and BPA congeners and β-scission to generate seven brominated products. All of these products were finally completely removed from reaction solution. Moreover, titanomagnetite showed excellent stability and reusability in heterogeneous UV/Fenton reaction. Heterogeneous UV/Fenton reaction catalyzed by titanomagnetite may be a novel and promising approach for the treatment of wastewater containing TBBPA and homologous persistent organic pollutants.

Acknowledgments

This is contribution no. IS-1522 from GIGCAS. We would like to thank Beijing Synchrotron Radiation Facility (BSRF) for providing us the beam time for the XANES measurement. This work was financially supported by the National Natural Science Foundation of China (Grant Nos. 41172045, 40773060 and 41103056).

Appendix A. Supplementary material

Supplementary material associated with this article can be found, in the online version, at http://dx.doi.org/10.1016/j.watres.2012.06.025.

REFERENCES

Abdallah, M.A.E., Harrad, S., Covaci, A., 2008. Hexabromocyclododecanes and tetrabromobisphenol-A in indoor air and dust in Birmingham, UK: implications for human exposure. Environmental Science & Technology 42 (18), 6855–6861.

Anipsitakis, G.P., Dionysiou, D.D., 2004. Transition metal/UV-based advanced oxidation technologies for water decontamination. Applied Catalysis B: Environmental 54 (3), 155–163.

Anpo, M., Che, M., Fubini, B., Garrone, E., Giamello, E., Paganini, M.C., 1999. Generation of superoxide ions at oxide surfaces. Topics in Catalysis 8 (3–4), 189–198.

Bangun, J., Adesina, A.A., 1998. The photodegradation kinetics of aqueous sodium oxalate solution using TiO_2 catalyst. Applied Catalysis A: General 175 (1–2), 221–235.

Barontini, F., Cozzani, V., Marsanich, K., Raffa, V., Petarca, L., 2004. An experimental investigation of tetrabromobisphenol A decomposition pathways. Journal of Analytical and Applied Pyrolysis 72 (1), 41–53.

Birnbaum, L.S., Staskal, D.F., 2004. Brominated flame retardants: cause for concern? Environmental Health Perspectives 112 (1), 9–17.

Blazso, M., Czegeny, Z., Csoma, C., 2002. Pyrolysis and debromination of flame retarded polymers of electronic scrap studied by analytical pyrolysis. Journal of Analytical and Applied Pyrolysis 64 (2), 249–261.

Borojovich, E.J.C., Aizenshtat, Z., 2002. Thermal behavior of brominated and polybrominated compounds II: pyroproducts of brominated phenols as mechanistic tools. Journal of Analytical and Applied Pyrolysis 63 (1), 129–145.

Burns, R.G., 1981. Intervalence transitions in mixed-valence minerals of iron and titanium. Annual Review of Earth and Planetary Sciences 9, 345–383.

Cariou, R., Antignac, J.P., Marchand, P., Berrebi, A., Zalko, D., Andre, F., Le Bizec, B., 2005. New multiresidue analytical method dedicated to trace level measurement of brominated flame retardants in human biological matrices. Journal of Chromatography A 1100 (2), 144–152.

Chen, J.X., Zhu, L.Z., 2007. UV-Fenton discolouration and mineralization of orange II over hydroxyl-Fe-pillared bentonite. Journal of Photochemistry and Photobiology A: Chemistry 188 (1), 56–64.

Chen, Q.Q., Wu, P.X., Dang, Z., Zhu, N.W., Li, P., Wu, J.H., Wang, X.D., 2010. Iron pillared vermiculite as a heterogeneous photo-Fenton catalyst for photocatalytic degradation of azo dye reactive brilliant orange X-GN. Separation and Purification Technology 71 (3), 315–323.

Chignell, C.F., Han, S.K., Bilski, P., Karriker, B., Sik, R.H., 2008. Oxidation of flame retardant tetrabromobisphenol A by singlet oxygen. Environmental Science & Technology 42 (1), 166–172.

Chong, M.N., Jin, B., Chow, C.W.K., Saint, C., 2010. Recent developments in photocatalytic water treatment technology: a review. Water Research 44 (10), 2997–3027.

Daneshvar, N., Salari, D., Khataee, A.R., 2003. Photocatalytic degradation of azo dye acid red 14 in water: investigation of the effect of operational parameters. Journal of Photochemistry and Photobiology A: Chemistry 157 (1), 111–116.

De Laat, J., Gallard, H., 1999. Catalytic decomposition of hydrogen peroxide by Fe(III) in homogeneous aqueous solution: mechanism and kinetic modeling. Environmental Science & Technology 33 (16), 2726–2732.

Eriksson, J., Rahm, S., Green, N., Bergman, A., Jakobsson, E., 2004. Photochemical transformations of tetrabromobisphenol A and related phenols in water. Chemosphere 54 (1), 117–126.

Fukushima, M., Ishida, Y., Shigematsu, S., Kuramitz, H., Nagao, S., 2010. Pattern of oxidation products derived from tetrabromobisphenol A in a catalytic system comprised of iron(III)-tetrakis(p-sulfophenyl)porphyrin, $KHSO_5$ and humic acids. Chemosphere 80 (8), 860–865.

Gasmi, A., Boudard, M., Zemni, S., Hippert, F., Oumezzine, M., 2009. Influence of non-magnetic Ti^{4+} ion doping at Mn site on structural and magnetic properties of $La_{0.67}Ba_{0.33}MnO_3$. Journal of Physics D: Applied Physics 42 (22), 225408–225414.

Guo, C.C., Liu, X.Q., Liu, Y., Liu, Q., Chu, M.F., Zhang, X.B., 2003. Studies of simple mu-oxo-bisiron(III)porphyrin as catalyst of cyclohexane oxidation with air in absence of cocatalysts or coreductants. Journal of Molecular Catalysis A: Chemical 192 (1–2), 289–294.

Han, S.K., Bilski, P., Karriker, B., Sik, R.H., Chignell, C.F., 2008. Oxidation of flame retardant tetrabromobisphenol A by singlet oxygen. Environmental Science & Technology 42 (1), 166–172.

Horikoshi, S., Miura, T., Kajitani, M., Horikoshi, N., Serpone, N., 2008. Photodegradation of tetrahalobisphenol-A (X = Cl, Br) flame retardants and delineation of factors affecting the process. Applied Catalysis B: Environmental 84 (3–4), 797–802.

Hornung, A., Balabanovich, A.I., Donner, S., Seifert, H., 2003. Detoxification of brominated pyrolysis oils. Journal of Analytical and Applied Pyrolysis 70 (2), 723–733.

Jing, L.Q., Sun, X.J., Xin, B.F., Wang, B.Q., Cai, W.M., Fu, H.G., 2004. The preparation and characterization of La doped TiO_2 nanoparticles and their photocatalytic activity. Journal of Solid State Chemistry 177 (10), 3375–3382.

Kitamura, S., Jinno, N., Ohta, S., Kuroki, H., Fujimoto, N., 2002. Thyroid hormonal activity of the flame retardants tetrabromobisphenol A and tetrachlorobisphenol A. Biochemical and Biophysical Research Communications 293 (1), 554–559.

Kwan, W.P., Voelker, B.M., 2002. Decomposition of hydrogen peroxide and organic compounds in the presence of dissolved iron and ferrihydrite. Environmental Science & Technology 36 (7), 1467–1476.

Lee, H.J., Kim, G., Kim, D.H., Kang, J.S., Zhang, C.L., Cheong, S.W., Shim, J.H., Lee, S., Lee, H., Kim, J.Y., Kim, B.H., Min, B.I., 2008. Valence states and occupation sites in $(Fe, Mn)_3O_4$ spinel oxides investigated by soft X-ray absorption spectroscopy and magnetic circular dichroism. Journal of Physics: Condensed Matter 20 (29), 2952031–2952035.

Li, D., Haneda, H., Hishita, S., Ohashi, N., 2005a. Visible-light-driven N-F-codoped TiO_2 photocatalysts. 2. Optical characterization, photocatalysis, and potential application to air purification. Chemistry of Materials 17 (10), 2596–2602.

Li, D., Haneda, H., Labhsetwar, N.K., Hishita, S., Ohashi, N., 2005b. Visible-light-driven photocatalysis on fluorine-doped TiO_2 powders by the creation of surface oxygen vacancies. Chemical Physics Letters 401 (4–6), 579–584.

Liang, X.L., Zhong, Y.H., Zhu, S.Y., Zhu, J.X., Yuan, P., He, H.P., Zhang, J., 2010a. The decolorization of Acid Orange II in non-homogeneous Fenton reaction catalyzed by natural vanadium-titanium magnetite. Journal of Hazardous Materials 181 (1–3), 112–120.

Liang, X.L., Zhu, S.Y., Zhong, Y.H., Zhu, J.X., Yuan, P., He, H.P., Zhang, J., 2010b. The remarkable effect of vanadium doping on the adsorption and catalytic activity of magnetite in the decolorization of methylene blue. Applied Catalysis B: Environmental 97 (1–2), 151–159.

Lin, K.D., Liu, W.P., Gan, J., 2009. Reaction of tetrabromobisphenol A (TBBPA) with manganese dioxide: kinetics, products, and pathways. Environmental Science & Technology 43 (12), 4480–4486.

Litter, M.I., 1999. Heterogeneous photocatalysis – transition metal ions in photocatalytic systems. Applied Catalysis B: Environmental 23 (2–3), 89–114.

Liu, H.M., Yang, W.S., Ma, Y., Cao, Y., Yao, J.N., Zhang, J., Hu, T.D., 2003a. Synthesis and characterization of titania prepared by using a photoassisted sol-gel method. Langmuir 19 (7), 3001–3005.

Liu, P., Kim, E.S., Kang, S.G., Jang, H.S., 2003b. Microwave dielectric properties of $Ca[(Li_{1/3}Nb_{2/3})_{1-x}Ti_{3x}]O_{3-\delta}$ ceramics with B_2O_3. Materials Chemistry and Physics 79 (2–3), 270–272.

Liu, X., Cheng, B., Hu, J.F., Qin, H.W., Jiang, M.H., 2008. Semiconducting gas sensor for ethanol based on $LaMg_xFe_{1-x}O_3$ nanocrystals. Sensors and Actuators B: Chemical 129 (1), 53–58.

Luo, S., Yang, S.G., Sun, C., Wang, X.D., 2011. Feasibility of a two-stage reduction/subsequent oxidation for treating tetrabromobisphenol A in aqueous solutions. Water Research 45 (4), 1519–1528.

Malik, P.K., 2004. Oxidation of safranine T in aqueous solution using Fenton's keagent: involvement of an Fe(III) chelate in the catalytic hydrogen peroxide oxidation of safranine T. Journal of Physical Chemistry A 108 (14), 2675–2681.

Moura, F.C.C., Oliveira, G.C., Araujo, M.H., Ardisson, J.D., Macedo, W.A.A., Lago, R.M., 2006. Highly reactive species formed by interface reaction between Fe^0-iron oxides particles: an efficient electron transfer system for environmental applications. Applied Catalysis A: General 307 (2), 195–204.

Muruganandham, M., Swaminathan, M., 2004. Decolourisation of reactive Orange 4 by Fenton and photo-Fenton oxidation technology. Dyes and Pigments 63 (3), 315–321.

Neyens, E., Baeyens, J., 2003. A review of classic Fenton's peroxidation as an advanced oxidation technique. Journal of Hazardous Materials 98 (1–3), 33–50.

Ngomsik, A.F., Bee, A., Draye, M., Cote, G., Cabuil, V., 2005. Magnetic nano- and microparticles for metal removal and environmental applications: a review. Comptes Rendus Chimie 8 (6–7), 963–970.

Pearce, C.I., Henderson, C.M.B., Telling, N.D., Pattrick, R.A.D., Charnock, J.M., Coker, V.S., Arenholz, E., Tuna, F., van der Laan, G., 2010. Fe site occupancy in magnetite-ulvospinel solid solutions: a new approach using X-ray magnetic circular dichroism. American Mineralogist 95 (4), 425–439.

Perez, M., Torrades, F., Domenech, X., Peral, J., 2002. Fenton and photo-Fenton oxidation of textile effluents. Water Research 36 (11), 2703–2710.

Pickup, D.M., Abou Neel, E.A., Moss, R.M., Wetherall, K.M., Guerry, P., Smith, M.E., Knowles, J.C., Newport, R.J., 2008. Ti K-edge XANES study of the local environment of titanium in bioresorbable TiO_2-CaO-Na_2O-P_2O_5 glasses. Journal of Materials Science-Materials in Medicine 19 (4), 1681–1685.

Ramankutty, C.G., Sugunan, S., Thomas, B., 2002. Study of cyclohexanol decomposition reaction over the ferrospinels, $A_{1-x}Cu_xFe_2O_4$ (A = Ni or Co and $x = 0$, 0.3, 0.5, 0.7 and 1), prepared by 'soft' chemical methods. Journal of Molecular Catalysis A: Chemical 187 (1), 105–117.

Ramirez, J.H., Maldonado-Hodar, F.J., Perez-Cadenas, A.F., Moreno-Castilla, C., Costa, C.A., Madeira, L.M., 2007. Azo-dye orange II degradation by heterogeneous Fenton-like reaction using carbon-Fe catalysts. Applied Catalysis B: Environmental 75 (3–4), 312–323.

Ronen, Z., Abeliovich, A., 2000. Anaerobic-aerobic process for microbial degradation of tetrabromobisphenol A. Applied and Environmental Microbiology 66 (6), 2372–2377.

Seda, T., Hearne, G.R., 2004. Pressure induced $Fe^{2+} + Ti^{4+} \rightarrow Fe^{3+} + Ti^{3+}$ intervalence charge transfer and the Fe^{3+}/Fe^{2+} ratio in natural ilmenite ($FeTiO_3$) minerals. Journal of Physics: Condensed Matter 16 (15), 2707–2718.

Simon, S.B., Sutton, S.R., Grossman, L., 2007. Valence of titanium and vanadium in pyroxene in refractory inclusion interiors and rims. Geochimica et Cosmochimica Acta 71 (12), 3098–3118.

Soderstrom, G., Marklund, S., 2002. PBCDD and PBCDF from incineration of waste-containing brominated flame retardants. Environmental Science & Technology 36 (9), 1959–1964.

Tryba, B., Piszcz, M., Grzmil, B., Pattek-Janczyk, A., Morawski, A.W., 2009. Photodecomposition of dyes on Fe-C-TiO_2 photocatalysts under UV radiation supported by photo-Fenton process. Journal of Hazardous Materials 162 (1), 111–119.

Utset, B., Garcia, J., Casado, J., Dom nech, X., Peral, J., 2000. Replacement of H_2O_2 by O_2 in Fenton and photo-Fenton reactions. Chemosphere 41 (8), 1187–1192.

Vicente, M.A., Iurascu, B., Siminiceanu, I., Vione, D., Gil, A., 2009. Phenol degradation in water through a heterogeneous photo-Fenton process catalyzed by Fe-treated laponite. Water Research 43 (5), 1313–1322.

Voordeckers, J.W., Fennell, D.E., Jones, K., Haggblom, M.M., 2002. Anaerobic biotransformation of tetrabromobisphenol A, tetrachlorobisphenol A, and bisphenol A in estuarine sediments. Environmental Science & Technology 36 (4), 696–701.

Wang, F., Smith, D.W., El-Din, M.G., 2003. Application of advanced oxidation methods for landfill leachate treatment: a review. Journal of Environmental Engineering and Science 2 (6), 413–427.

Wechsler, B.A., Lindsley, D.H., Prewitt, C.T., 1984. Crystal-structure and cation distribution in titanomagnetites ($Fe_{3-x}Ti_xO_4$). American Mineralogist 69 (7–8), 754–770.

de Wit, C.A., 2002. An overview of brominated flame retardants in the environment. Chemosphere 46 (5), 583–624.

Xu, J., Meng, W., Zhang, Y., Li, L., Guo, C.S., 2011. Photocatalytic degradation of tetrabromobisphenol A by mesoporous BiOBr: efficacy, products and pathway. Applied Catalysis B: Environmental 107 (3–4), 355–362.

Yang, S.J., He, H.P., Wu, D.Q., Chen, D., Liang, X.L., Qin, Z.H., Fan, M.D., Zhu, J.X., Yuan, P., 2009a. Decolorization of methylene blue by heterogeneous Fenton reaction using $Fe_{3-x}Ti_xO_4$ ($0 \le x \le 0.78$) at neutral pH values. Applied Catalysis B: Environmental 89 (3–4), 527–535.

Yang, S.J., He, H.P., Wu, D.Q., Chen, D., Ma, Y.H., Li, X.L., Zhu, J.X., Yuan, P., 2009b. Degradation of methylene blue by heterogeneous Fenton reaction using titanomagnetite at neutral pH values: process and affecting factors. Industrial & Engineering Chemistry Research 48 (22), 9915–9921.

Zepp, R.G., Faust, B.C., Hoigne, J., 1992. Hydroxyl radical formation in aqueous reactions (pH 3–8) of iron(II) with hydrogen-peroxide: the photo-Fenton reaction. Environmental Science & Technology 26 (2), 313–319.

Zhang, Y., Dou, X.M., Liu, J., Yang, M., Zhang, L.P., Kamagata, Y., 2007. Decolorization of reactive brilliant red X-3B by heterogeneous photo-Fenton reaction using an Fe-Ce bimetal catalyst. Catalysis Today 126 (3–4), 387–393.